

April 2000

Manganese surface segregation in NiMnSb

Delia Ristoiu

CNRS Laboratoire Louis Née 'l, 25 Avenue des Martyrs BP 166, 38042 Grenoble CEDEX 09, France

J. P. Nozie`res

CNRS Laboratoire Louis Née 'l, 25 Avenue des Martyrs BP 166, 38042 Grenoble CEDEX 09, France

C.N. Borca

University of Nebraska-Lincoln

B. Borca

University of Nebraska-Lincoln

Peter A. Dowben

University of Nebraska-Lincoln, pdowben@unl.edu

Follow this and additional works at: <http://digitalcommons.unl.edu/physicsdowben>

 Part of the [Physics Commons](#)

Ristoiu, Delia; Nozie`res, J. P. ; Borca, C.N.; Borca, B.; and Dowben, Peter A., "Manganese surface segregation in NiMnSb" (2000).

Peter Dowben Publications. 30.

<http://digitalcommons.unl.edu/physicsdowben/30>

This Article is brought to you for free and open access by the Research Papers in Physics and Astronomy at DigitalCommons@University of Nebraska - Lincoln. It has been accepted for inclusion in Peter Dowben Publications by an authorized administrator of DigitalCommons@University of Nebraska - Lincoln.

Manganese surface segregation in NiMnSb

Delia Ristoiu and J. P. Nozières

CNRS Laboratoire Louis Néel, 25 Avenue des Martyrs BP 166, 38042 Grenoble CEDEX 09, France

C. N. Borca, B. Borca, and P. A. Dowben^{a)}

Department of Physics and Astronomy and the Center for Materials Research and Analysis, Behlen Laboratory of Physics, University of Nebraska-Lincoln, Lincoln, Nebraska 68588-0111

(Received 21 December 1999; accepted for publication 25 February 2000)

A quantitative analysis of the surface composition of the Heusler alloy NiMnSb has been undertaken using angle-resolved x-ray photoemission spectroscopy and the surface composition characterized. With sufficient annealing cycles, the stoichiometric surface evolves to a surface that is manganese rich. This indicates that the surface enthalpy is different from the bulk for the Heusler alloy NiMnSb. © 2000 American Institute of Physics. [S0003-6951(00)00617-3]

The presence of surface segregation is an indicator of a difference in free energy (chemical potential) between the surface and the bulk in the absence of segregation.^{1,2} This difference in energy can be related to the creation of a surface electronic structure very different from the bulk, as has been noted for the complex oxides,²⁻⁴ as well as result in a surface lattice structure different from the bulk and, of course, become the driving force for segregation. In addition, defects and variations in the local lattice order are believed to strongly influence the net electron polarization in NiMnSb near the Fermi level.⁵

We have been able to establish that surface preparation has a profound effect upon the surface electronic structure and polarization in spin-polarized inverse photoemission for the Heusler alloy NiMnSb.⁶ The possibility of surface segregation has been suggested for NiMnSb.^{7,8} Bona *et al.* proposed that Sb segregation dominates the surface region.⁷ In fact, as we show in this letter, once the excess Sb protective capping layer is removed, Mn segregation dominates the surface and near surface region of NiMnSb.

The single crystal epitaxial thin film NiMnSb(100) samples were grown on a Mo(100) seed layer grown on chemically cleaned MgO(100) substrate. A 1000 Å Sb capping layer was deposited to prevent oxidation of the NiMnSb crystalline films prior to the surface sensitive measurements. Crystallinity and orientation of the NiMnSb was established by x-ray diffraction and, once the capping layers were removed, again by low-energy electron diffraction (LEED).

Angle-resolved x-ray photoemission spectroscopy (ARXPS) of the Sb, Mn, and Ni core levels was undertaken on a number of different samples. The elemental Ni ($2p_{3/2}$), Mn ($2p_{3/2}$ and $2p_{1/2}$), and Sb ($3d_{5/2}$ and $3d_{3/2}$) core levels and the intensities were measured, as were the binding energies, as a function of emission angle, with respect to the surface normal, using a (PHI Model 10-360 hemispherical energy analyzer).

Core level photoemission data are shown for NiMnSb in Fig. 1. The Mn $2p_{3/2}$ spectra from the NiMnSb samples and the LEED (insert to Fig. 1) indicate that the disorder is limited in the surface region. The full width at half maximum of the Mn $2p_{3/2}$ core level spectra is 5.3 to 5.8 eV as compared

to 4–4.5 eV for $\text{La}_{0.65}\text{Ca}_{0.35}\text{MnO}_3$ and $\text{La}_{0.65}\text{Sr}_{0.35}\text{MnO}_3$.⁹ The increase in the Mn $2p_{3/2}$ half width is consistent with the placement of Mn in a more metallic environment in half metallic NiMnSb than is the case in the half metallic manganese perovskites. (The core level line shape does not provide a good indicator as to the defect density in the surface region.)

Following different surface preparation procedures, we have plotted the emission angle dependent XPS core level intensity ratios in Fig. 2. The measured XPS intensity $I(\theta)$,

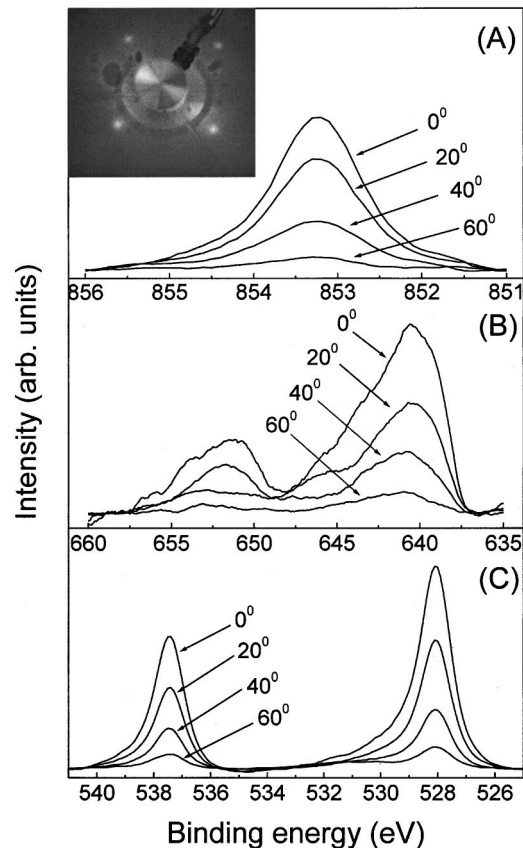


FIG. 1. The emission angle dependence of the x-ray photoemission data. The Ni $2p_{3/2}$ (A), Mn $2p_{3/2} + 2p_{1/2}$ (B), and Sb $3d_{5/2} + 3d_{3/2}$ (C) core levels of NiMnSb are shown as a function of emission angle, as indicated. The LEED pattern of the stoichiometric surface for NiMnSb, obtained at an electron energy of 34 eV is shown in the inset.

^{a)}Electronic mail: pdowben@unl.edu

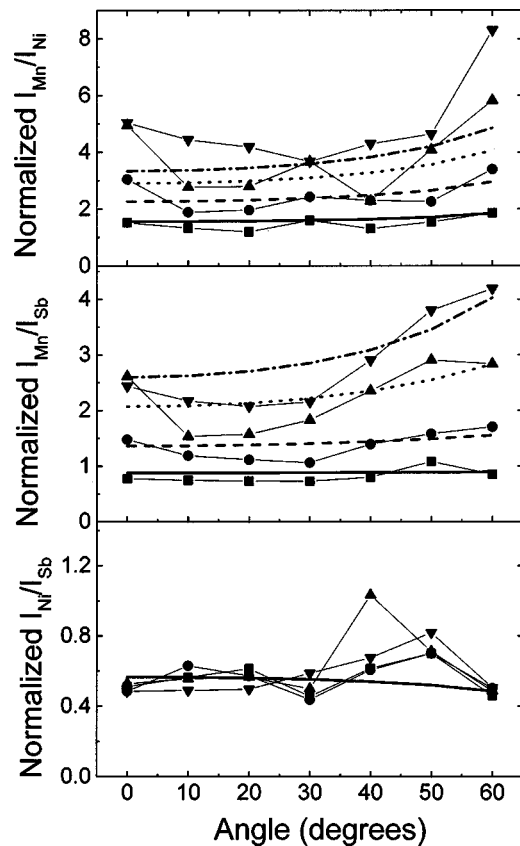


FIG. 2. The angle resolved x-ray photoemission intensity ratios of the Ni $2p_{3/2}$, Mn $2p_{3/2}$, and Sb $3d_{5/2}$ core levels of NiMnSb. The data are compiled from spectra were taken as a function of emission angle following removal of the excess Sb with a 700 K anneal (■) and following continued sputtering and annealing cycles of 10 min (●) followed by 1/2 h (▲) and finally by 1 h (▼) total annealing times. The data points are fitted with a segregation model in which Mn atoms migrate to both vacancy sites as well as replace Sb and Ni atoms from their lattice sites in the surface region except for data for the surface stoichiometric alloy termination MnSb (surface):Ni: (MnSb:Ni)_n. The details of the Mn concentration profiles used to model the data are shown in Fig. 3(a).

for the different elemental core levels ($2p_{3/2}$ for Ni and Mn, $3d_{5/2}$ for Sb) is normalized by the cross section for the different elemental core levels and the transmission factor. The normalized intensity ratio is thus given as

$$R(\theta) = \frac{I_A(\theta)/\sigma_A}{I_B(\theta)/\sigma_B} \left[\frac{E_{\text{kin}}^p(A) - C}{E_{\text{kin}}^p(B) - C} \right], \quad (1)$$

where θ is the emission angle with respect to the surface normal, σ_A , σ_B are the cross sections [using the calculations by Scofield for an excitation energy of 1253.6 eV (Mg $K\alpha$)]¹⁰ and the term $E_{\text{kin}}^p(A) - C$ corrects for the transmission of the electron energy analyzer at the kinetic energy of core level A. Based on the measured transmission functions for this type of analyzer,¹¹ we have set $p=0.5$, $C=0$.

A procedure that results in the preparation of the stoichiometric or near stoichiometric ordered alloy surface, terminating in MnSb, was outlined previously.⁶ Ar⁺ sputtering (to remove surface contamination) followed by a flash anneal to 700 K (to remove the excess Sb) results in one of the normalized XPS intensity ratios sets shown in Fig. 2. This surface exhibits a sharp LEED pattern (as seen in the inset to Fig. 1), with a 6.0 ± 0.1 Å surface lattice constant consistent with the 5.9 Å unit cell of NiMnSb.

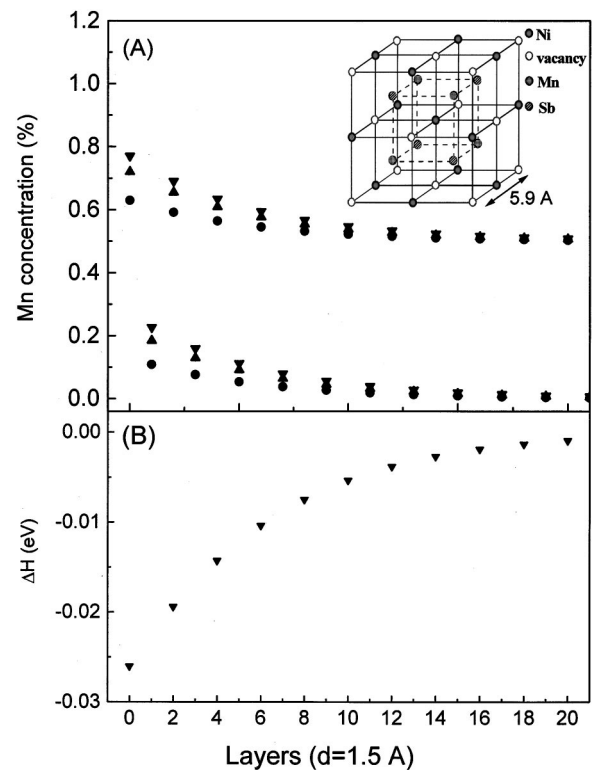


FIG. 3. The concentration of Mn in the near surface region obtained from fits from the angle resolved x-ray photoemission data are shown in panel (a). The odd layers are Mn/Ni. The Mn concentration profiles denoted by the different symbols (●▲▼) are fit to the data shown by similar symbols in Fig. 2. The energy difference between the surface and the bulk based on the most extensive Mn segregation is shown in panel (b). The inset shows the crystal structure of NiMnSb.

As previously noted,⁶ the surface of NiMnSb is fragile and Mn segregation readily occurs, as indicated by the angle resolved x-ray photoemission shown in Fig. 2. With continued annealing (and sputtering to remove surface contamination), there is a clear sequence of increasing Mn/Sb and Mn/Ni ratios, though the Ni/Sb core level intensity ratio is largely preserved.

The different sets of data can be analyzed using a previously applied semi-empirical method^{1,2} to give a more quantitative picture of the extent of surface segregation. Quantitative analysis of the data makes use of the decrease in the effective mean free path of the escaping electrons with increasing emission angle.^{1,2} A summation is undertaken to account for each layer contributing to the photoemission signal. NiMnSb has, effectively, a layered crystal structure (inset to Fig. 3) with alternate Mn–Sb and Ni–vacancy layers, with the distance between layers approximately $d = a_{\text{NiMnSb}}/4 = 1.5$ Å. The various models for surface termination with no segregation would have $f_j(A)$, $f_j(B) = 1/2$ or zero depending upon the layer considered, for components A and B (since we have two elements per layer). Thus, for the constituent component A, with concentration $f_j(A)$, the normalized core level intensities can be written with respect to a reference constituent component B, as

$$R(\theta) = \frac{\sum_{j=0}^{\infty} f_j(A) e^{-jd[\lambda_A \cos(\theta)]}}{\sum_{j=0}^{\infty} f_j(B) e^{-jd[\lambda_B \cos(\theta)]}}, \quad (2)$$

where λ_{Ni} (7 Å for the Ni $2p_{3/2}$ core), λ_{Mn} (9.35 Å for the

Mn $2p$ cores), and λ_{Sb} (10.8 Å for the Sb $3d$ cores) are the effective mean free paths, adapted from the calculated mean free paths of Penn.¹² The surface, with the Sb cap removed and little additional annealing, can be modeled using Eq. (2). We find that models that have the surface terminate in NiSb or NiMn do not fit the data nearly as well as the model based upon the stoichiometric alloy terminating in MnSb at the surface.⁶

$$R(\theta) = \frac{\sum_{j=0}^{\infty} \left\{ \frac{1}{2} e^{-[(2j+1)d]/[\lambda_A \cos(\theta)]} + \delta e^{-(2j/G)} e^{-(2jd)/[\lambda_A \cos(\theta)]} \right\}}{\sum_{j=0}^{\infty} \frac{1}{2} e^{-(2j+\xi)d/[\lambda_B \cos(\theta)]}}, \quad (3)$$

where the parameters δ and G are the segregation to the topmost ($j=0$) layer (above the terminal MnSb layer) and the segregation depth in units of the distance d between layers, respectively. Thus MnSb layers are the odd numbered layers and Ni plus segregated Mn occupy even layers except for the zeroth layer which contains only Mn segregation. Alternatively Mn can segregate to both vacancy sites as well as replace both Sb and Ni, in this scheme

$$R(\theta) = \frac{\sum_{j=0}^{\infty} \left(\exp\left[\frac{-2jd}{\lambda_A \cos(\theta)}\right] + \delta \left\{ \exp\left[\frac{-2j}{G} + \frac{-2jd}{\lambda_A \cos(\theta)}\right] + \exp\left[\frac{-(2j+1)}{G} + \frac{-(2j+1)d}{\lambda_A \cos(\theta)}\right] \right\} \right)}{\sum_{j=0}^{\infty} \left\{ \exp\left[\frac{-(2j+\xi)d}{\lambda_B \cos(\theta)}\right] - \delta \exp\left[\frac{-(2j+\xi)}{G} + \frac{-(2j+\xi)d}{\lambda_B \cos(\theta)}\right] \right\}}. \quad (4)$$

So $\xi=1$ for Ni the reference and $\xi=0$ for Sb the reference. The surfaces exhibiting the larger Mn/Sb and Mn/Ni ratios can be modeled if Mn segregation is considered, using (4), as seen in Fig. 2 by the solid line indicating the model fits. The model fits to the data are shown in Fig. 3(a) and compared to the experimental data (following increasingly extensive segregation) in Fig. 2.

From the fits to the data, we have constructed Mn concentration profiles [see Fig. 3(a)] from the surface to the bulk using the formulas $f_i(\text{Mn}) = b + \delta(\exp -j/G)$, where $b=1/2$ for the MnSb layers and $b=0$ for the Ni layers. With increased annealing (and sputtering) at 700 K, the changing core level intensity ratios can be roughly modeled by Mn segregation to the surface, Mn segregation to the vacancy sites, and Mn segregation possibly leading to the displacement of atoms for the extensively annealed sample, as shown in Fig. 3(a) and indicated by the symbol (▼). The extensive annealing leads to formation of a different material from NiMnSb in the surface region. Because our model fits are not unique solutions to the data, the exact details of the surface structure with extensive annealing of NiMnSb will require other, surface sensitive, structural studies.

The substantial surface segregation implies an energy difference (in the absence of segregation).¹³ This has been calculated from the segregation profiles, as in Fig. 3(b) using the approximation that $f_j(A)/f_j(B) = [f_b(A)/f_b(B)] \exp(-\Delta H/k_B T)$, where $f_b(A)$ and $f_b(B)$ are the bulk layer concentrations of constituents A and B , and T is the annealing temperature.

The extensive segregation of manganese would reduce the measured polarization of the surface given the influence of atomic disorder on the electronic structure.⁵ The observed

Because the core level photoemission intensity ratios change with increased annealing, as seen in Fig. 2, the models for the core level intensity must include the possibility of segregation. For Mn segregation, we postulate that Mn segregation to the surface and to the vacancy sites within the Ni layers are both possible. To account for this type of segregation we have fit the data in Fig. 2 with the normalized intensity ratio of Mn to a reference constituent B rewritten as

segregation, noted here, is very consistent with marked decline in polarization measured in spin-polarized inverse photoemission following extensive segregation⁶ as well as in spin-polarized tunneling measurements.¹⁴

This work was supported by NSF through Grant No. DMR-98-02126, the Center for Materials Research and Analysis (CMRA), the Nebraska Research Initiative at the University of Nebraska, and the Region Rhone-Alpes through the "Nanotechnologie" program under Contract No. PR97024.

¹ *Surface Segregation Phenomena*, edited by P. A. Dowben and A. Miller (CRC Press, Boston, 1990), p. 145.

² J. Choi, C. Waldfried, S.-H. Liou, and P. A. Dowben, *J. Vac. Sci. Technol. A* **16**, 2950 (1998); J. Choi, J. Zhang, S.-H. Liou, P. A. Dowben, and E. W. Plummer, *Phys. Rev. B* **59**, 13453 (1999).

³ S. H. Liu and R. A. Klemm, *Phys. Rev. Lett.* **73**, 1019 (1994).

⁴ M. Lindroos and A. Bansil, *Phys. Rev. Lett.* **75**, 1182 (1995).

⁵ D. Orgassa, H. Fujiwara, T. C. Schulthess, and W. H. Butler, *Phys. Rev. B* **60**, 13237 (1999).

⁶ D. Ristoiu, J. P. Nozières, C. N. Borca, T. Komesu, H. K. Jeong, and P. A. Dowben, *Europhys. Lett.* (in press).

⁷ G. L. Bona, F. Meier, M. Taborelli, E. Bucher, and P. H. Schmidt, *Solid State Commun.* **56**, 391 (1985).

⁸ J.-H. Park, E. Vescovo, H.-J. Kim, C. Kwon, R. Ramesh, and T. Venkatesan, *Nature (London)* **392**, 794 (1998).

⁹ J. Choi, H. Dulli, S.-H. Liou, P. A. Dowben, and M. A. Langell, *Phys. Status Solidi B* **214**, 45 (1999).

¹⁰ J. H. Scofield, *J. Electron Spectrosc. Relat. Phenom.* **8**, 129 (1976).

¹¹ M. P. Seah, M. E. Jones, and M. T. Anthony, *Surf. Interface Anal.* **6**, 242 (1984); M. P. Seah, *ibid.* **20**, 243 (1993).

¹² D. R. Penn, *J. Electron Spectrosc. Relat. Phenom.* **9**, 29 (1976).

¹³ S. Y. Liu and H. H. Kung, *Surf. Sci.* **110**, 504 (1981).

¹⁴ C. T. Tanaka, J. Nowak, and J. S. Mooder, *J. Appl. Phys.* **86**, 6239 (1999).